LABORATORY SCIENCE

Four corneal presbyopia corrections: Simulations of optical consequences on retinal image quality

Tobias Koller, MD, Theo Seiler, MD, PhD

PURPOSE: To investigate the possibility of multifocal or aspherical treatment of the cornea with optical ray tracing.

SETTING: Institute for Refractive and Ophthalmic Surgery, Zurich, Switzerland.

METHODS: The optical consequences of 4 corneal shapes—global optimum (GO) for curvature and asphericity, central steep island (CSI), decentered steep island (DSI), and centered steep annulus (CSA)—for presbyopia correction were analyzed using a modified Liou-Brennan eye model and ray tracing with a commercial optic design software (Zemax, Zemax Development Corp.). The ocular optical configuration for far vision was a point light source at a distance of 5 m, 1 degree up, and a pupil diameter of 5.0 mm and for near vision, 0.4 m distance, 1 degree up, and a pupil diameter of 2.5 mm. The curvature radius (R) of the cornea and its asphericity (Q) were used as operands to optimize (simultaneously for near and far vision) the quality of the retinal image described by means of the minimum spot diameter or the root-mean-square (RMS) wavefront error.

RESULTS: Starting from an emmetropic eye optimized for R and Q, the RMS wavefront error in the retina was 0.07 μm (far) and 1.42 μm (near). The GO resulted in a wavefront error of 1.42 μm (far) and 0.52 μm (near); improvement of near vision using reading glasses is possible. The CSI yielded 0.91 μm (far) and 0.13 μm (near); spectacles did not improve far or near vision. The DSI and CSA had significantly worse results for near and far vision.

CONCLUSIONS: Of the options studied, GO and CSI seemed the most promising alternatives for corneal presbyopia correction. Although reading glasses can improve near vision in GO, reading glasses did not improve near vision in CSI-treated eyes. The CSI treatment is critically dependent on centration and a reverse treatment is difficult to achieve.

J Cataract Refract Surg 2006; 32:2118–2123 © 2006 ASCRS and ESCRS

Optical approaches to presbyopia include reading glasses, monovision, multifocal contact lenses and intraocular lenses (IOLs), and accommodating IOLs. None can restore accommodation, but all are compromises that establish relatively fair quality of near vision at the expense of good far vision. Even a small amount of astigmatism provides some pseudoaccommodation in pseudophakic patients.[1] Several methods to restore accommodation with scleral expansion near the ciliary body were designed; however, none is proven effective.[2–4]

In refractive laser surgery, the first "presbyopia corrections" date to the early 1990s[5,6] and have not gained clinical acceptance. More sophisticated presbyopia correction profiles have been proposed (mostly as patents) including an induced central steep island (CSI),[7,8] decentered steep area,[9,10] and a near vision zone in the midperiphery of the cornea[11,12] (Figure 1). Although the approaches are different, the preliminary results look promising[10,12]; however, we are not aware of reports of the expected loss of quality of vision that accompany this type of multifocal treatment.

This study examined theoretically some of these proposals by means of optical ray tracing and looked for optimum strategies to create an aspherical or multifocal corneal surface that facilitates near vision in presbyopia and minimizes distance vision side effects.

0886-3350/06/$-see front matter
doi:10.1016/j.jcrs.2006.08.038

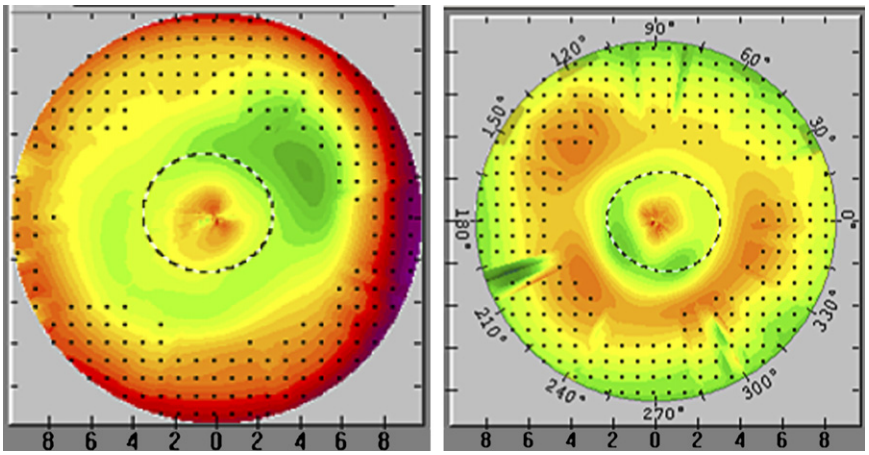

Figure 1. Corneal topographies of eyes with induced multifocal corneas. *Left*: Central steep island. *Right*: Centered steep annulus.

MATERIALS AND METHODS

Theoretical Eye Model

The eye model used here is based on the model of Liou and Brennan.[13] This model is characterized by aspherical anterior and posterior corneal and lenticular surfaces. In addition, it includes a linear refractive index gradient of $\Delta n = 0.2$ inside the lens. The parameters for the emmetropic eye are shown in Table 1. The optical surfaces were approximated by a conoid surface

$$z = (x^2/R + y^2/R)/\left\{1 + [1 - (1+Q)(x^2+y^2)/R^2]^{1/2}\right\}$$

where 1/R is the curvature and Q is the asphericity constant, the positive z direction points into the eye, the positive y direction upward. The reference wavelength was 555 nm. To include the Stiles-Crawford effect,[14] a transmission filter was introduced

$$T(r) = \exp(-ar^2)$$

with the apodization constant $a = 0.105$ and $r =$ the radial distance from the center of the pupil. To model central or decentered steep islands and annuli, cubic spline functions were introduced in steps of 0.5 mm radial distance from the apex of the cornea. All optical surfaces were centered on the optical axis.

Based on mesopic pupil diameters in the age group of interest,[15] a pupil diameter of 5.0 mm was assumed for simulation of the far distance vision configuration (object distance 5 m). The reported accommodative constriction of the pupil (pupillary near reflex) ranges from 0.15 to 1.6 mm per diopter of accommodation stimulation,[16,17] and this effect seems not to decrease with age, also remaining active in presbyopic subjects unable to accommodate.[18] For the near vision configuration (object distance 0.4 m), therefore, a pupil diameter of 2.5 mm was assumed.

The object was a point light source located 1 degree up. Additional (reading) glasses had a distance of 12.0 mm from the vertex of the cornea.

Because there is no universally accepted metric of quality of the retinal image,[19] the simplest metrics available were used, the root-mean-square (RMS) spot diameter or the RMS wavefront error.[20]

All calculations were performed with the optical design program Zemax EE, version March 2004 (Zemax Development Corp.). When not otherwise stated, the optimization processes were aimed at a minimum spot diameter in the retina (circle of least confusion); however, depending on the problem, modulation transfer function and wavefront error were also used as optimization operands.

The quality of the retinal image was determined in near and far distance configuration for the following scenarios: (1) the emmetropic eye optimized regarding asphericity and eye length; (2) the global optimum (GO) for simultaneous near and far distance vision optimized regarding R and Q; (3) CSI with a diameter of 3.0 mm and an additional corneal refractive power of 3.00 diopters (D) optimized regarding R and Q; (4) scenario 3, but the CSI is decentered toward inferior in 0.5 mm steps up to 3.0 mm; (5) centered steep annulus with a diameter of 3.0 mm and an additional corneal refractive power of 3.00 D (Table 2).

Table 1. Parameters of the optimized emmetropic eye model.

Surface	Curvature Radius (R) (mm)	Asphericity (Q) (mm)	Apex Position	Refractive Index
Anterior cornea	7.77	−0.158	0.00	1.376
Posterior cornea	6.40	−0.60	0.52	1.336
Pupil	13.00	0.00	3.68	1.336
Anterior lens	12.40	−0.94	3.68	1.453*
Posterior lens	−8.10	0.96	7.70	1.336
Retina	12.00	0.00	24.01	—

*The lens includes a linear gradient of refractive index increasing from 1.453 at the surfaces to 1.652 in the center.

Accepted for publication August 1, 2006.

From the Institut für Refraktive und Ophthalmo-Chirurgie (IROC), Zürich, Switzerland.

Dr. Seiler is a consultant to WaveLight. Dr. Koller has no financial or proprietary interest in any material or method mentioned.

Corresponding author: Theo Seiler, MD, PhD, Institut für Refraktive und Ophthalmo-Chirurgie (IROC), Stockerstrasse 37, CH-8002 Zürich, Switzerland. E-mail: info@iroc.ch.

Table 2. Quality of the retinal image (point light source, λ = 550 nm).

Optical Scenario	RMS Wavefront Error (Minimum Spot Diameter) (μm)			
	Far Distance/5.0 m		Near Distance/0.4 m	
Emmetropic eye optimized (Q = −0.158)	0.07	(1.40)	1.42	(75.48)
Global optimum for R and Q (R = 7.55; Q = −0.68)	1.42	(37.60)	0.52	(34.20)
Central steep island optimized R and Q (R = 7.92 ; Q = +0.22)	0.91	(44.50)	0.13	(17.60)
Decentered steep island, decentered by 1.0 mm, optimized R and Q (R = 7.68; Q = −0.42)	2.75	(82.90)	1.29	(76.30)
Centered steep annulus optimized R and Q (R = 7.21; Q = −1.72)	3.54	(130.10)	1.21	(77.62)

RMS = root mean square

RESULTS

Optimization of eye length and asphericity in the emmetropic eye for far distance vision yielded approximately physiologic values (Table 1): an eye length of 24.01 mm and a corneal asphericity constant of −0.158. The minimum spot diameter in the retina d = 1.396 μm as well as the RMS wavefront error of 0.07 μm were close to the diffraction limit and significantly smaller than the physiologic higher-order wavefront errors measured in a normal population, which amount to approximately 0.33 μm ± 0.1 (SD).

Comparing the image planes close to the retina for the far and near distance object revealed in the emmetropic eye (no accommodation) a shift of the focus of 890 μm behind the retina (Figure 2), which could be shifted back into the retina by a reading glass of 2.32 D with a vertex distance of 12.0 mm.

Figure 3 shows the RMS wavefront error through the retina for the GO regarding R and Q in the far and near object configuration. The 2 configurations differed not only by the distance of the object but also by the pupil diameter. The RMS wavefront error in the retina increased to 1.42 μm for the far distance object and decreased to 0.52 μm for the near object (Table 2). Comparing the optimized emmetropic eye (scenario 1) with the GO (scenario 3), the difference consisted of an increase in central corneal power of 1.40 D (myopia) and a more prolate corneal shape, Q_{GO} = −0.68. Again, by using a reading glass of 1.01 D, the focus could be shifted into the retina, minimizing the RMS wavefront error in the retina to 0.03 μm.

The spot diameter through the retina for the CSI with optimized R and Q for simultaneous far and near vision is shown in Figure 4. Whereas for the far distance object, the spot diameter was comparable to that in GO, it was better by a factor of approximately 2 to 3 for near vision. However, reading glasses could not improve this result further.

Decentration of the steep island degraded the quality of the retinal image (Figure 5). Compared to the CSI, a decentration of, for example, 1.0 mm resulted in a 1.6-fold worsening for far and 4.7-fold worsening for near vision. Again, reading glasses marginally improved near vision.

Finally, the centered annulus with a "near" zone in the midperiphery of the cornea resulted in significant degradation of the retinal image for near and far distance objects (Table 2) with no chance to improve near vision with reading glasses.

DISCUSSION

The major finding of this theoretical study was that there are configurations of the corneal shape that represent

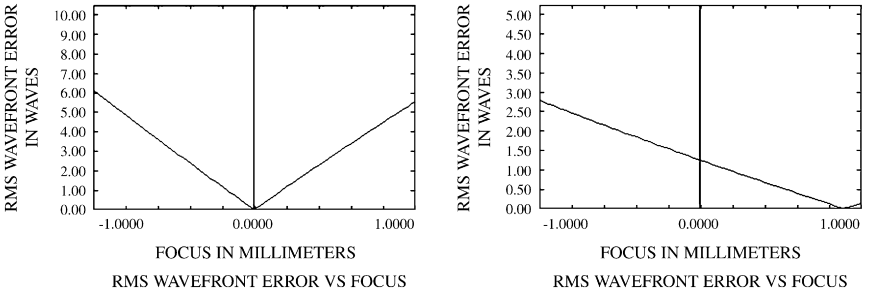

Figure 2. The RMS wavefront error as a function of the position in front of and behind the retina in the emmetropic nonaccommmodated eye. The focus in the far distance configuration is located in the retina (*left*); in the near configuration it is shifted 900 μm behind the retina (*right*).

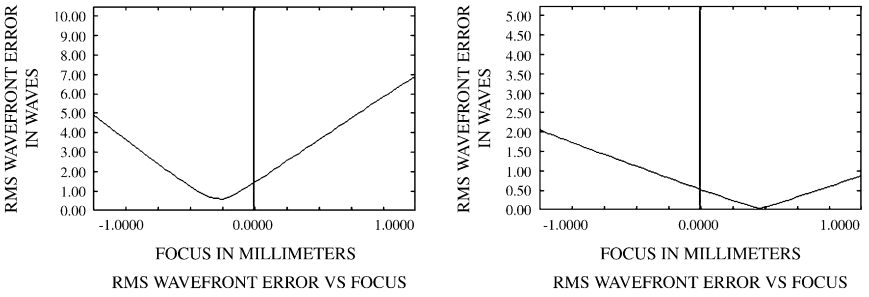

Figure 3. The RMS wavefront error as a function of the position near the retina with the GO regarding R and Q. Compared to the emmetropic eye, the wavefront error for far distance vision (*left*) has increased; however, in the near configuration, the focus (*right*) is located only 400 μm behind the retina and may be shifted into the retina level by means of reading glasses.

a clinically meaningful compromise of minor losses in far distance vision with improvement in near vision. Of the 4 options studied, the 2 most attractive approaches are the (1) CSI combined with appropriate curvature and asphericity in the rest of the cornea and (2) GO for curvature and asphericity. Whereas the first proposal means a multifocal cornea with 2 main foci, the second is a purely aspherical hyperprolate shape creating a small amount of myopia with increased depth of focus. Both corneal shapes provide a stronger refractive power for near in the central area surrounded by a midperiphery with less power. The 2 main driving forces of the multifocal CSI, as well as the aspheric GO shape, are on one hand the pupil size that decreases during focusing near objects (pupillary near reflex) and, on the other hand, the depth of focus that increases in both optical scenarios.

With the pupil near reflex in mind as a main driving force and given the high variation in pupil diameter between individuals, it is obvious that the pupil dynamics gain extraordinary importance when dealing with corneal presbyopia corrections. Modeling only 2 fixed pupil sizes (5.0 mm for far and 2.5 mm for near fixation) does not reflect the reality. Table 3 lists the RMS wavefront errors in the retinal level for different pupil diameter combinations. In general, the optical quality of the retinal image of distant objects is not much affected by pupil diameters ranging from 4.0 to 6.0 mm; however, near objects are better imaged the smaller the pupil is. This is not a surprising result because smaller pupils give better depth of focus.

The CSI configuration is a corneal analogue to the artificial bifocal IOL[21] with all its known advantages and disadvantages, such as loss in contrast sensitivity, halos, glare, and reduced visual satisfaction.[22–24] In contrast, the aspheric GO includes an even naturally occurring corneal asphericity that provides a variable pseudoaccommodation depending on the asphericity constant Q and the pupil diameter change amplitude during the near reflex.

Because of its increased depth of focus, the advantage of the CSI is a 2 to 3 times better retinal image of near objects than with the GO shape and at least 4-fold better than with the nonaccommodated emmetropic eye. Due to the increased depth of focus, a disadvantage is the inability to improve both near and far vision with spectacles. In addition, the effect of the CSI is critically dependent on centration (Figure 5): At a decentration of 0.1 mm, the advantage of the CSI compared with GO is gone and a degradation of the retinal images for distance and near vision occurs. Using modern eye trackers, centration is achieved reliably; however, there is a principal problem because the CSI should be centered regarding the visual axis and the crossing point of the visual axis through the cornea is uncertain and hard to determine. Reasonable centration is more easily obtained with the GO approach because it does not contain such a localized optical inhomogeneity.

A major disadvantage of multifocal optics of the eye is the loss in mesopic vision, measured in low-contrast visual acuity and contrast sensitivity. After multifocal IOL implantation[22,24–26] many patients report an increase in halos.[23] Regarding these optical side effects, we would like to cite a recent statement of Baïkoff et al.[27]: "Optical defects are inevitable with multifocal IOLs…." Although this argument holds mainly for a cornea that has a clearly multifocal CSI shape, a similar loss in contrast sensitivity is expected with strongly aspherical corneas. However, an asphericity

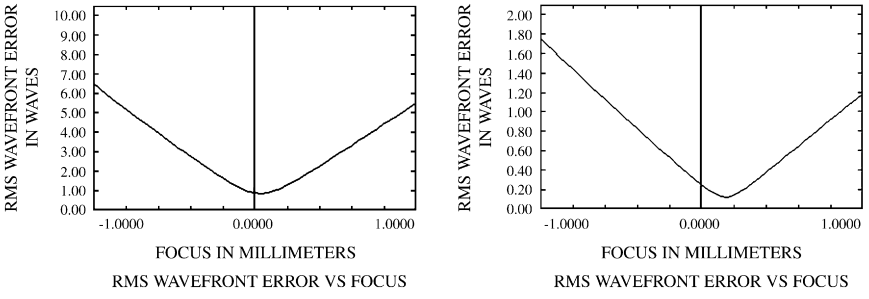

Figure 4. The RMS wavefront error as a function of the position near the retina with a CSI 3.0 mm in diameter and an additional refractive corneal power of 3.00 D. The image plane for near vision (*right*) is closer to the retina level than the GO, with the advantage of a better near vision and the disadvantage of no chance of improvement with glasses.

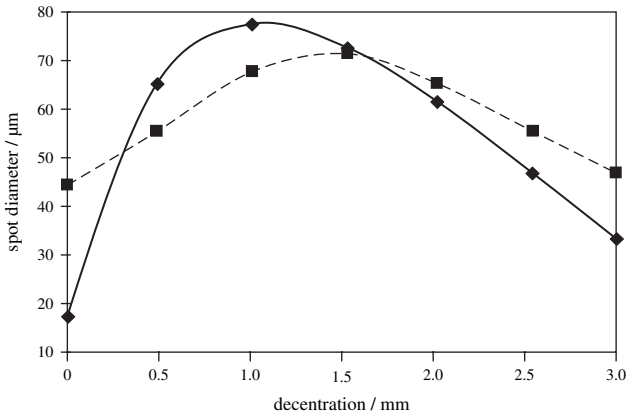

Figure 5. Decentration of the steep island degrades the quality of the retinal image significantly more for near objects (*diamonds*) than for distance objects (*rectangles*).

constant Q of −0.7, as intended in the GO, is only −0.5 away from the mean[28] and compares favorably with the up to 3 times larger changes in the asphericity constant after standard myopic laser in situ keratomileusis of up to +1.50 D.[29,30] Also, emmetropic or hyperopic eyes receiving a hyperopia correction for attempted slight myopia for monovision experience a shift in asphericity toward prolate of approximately −0.50 D.[31]

The most frequent presbyopia correction is the monovision approach, in which the dominant eye is corrected for emmetropia and the nondominant eye for mild myopia ranging from −0.50 D to −2.00 D.[32–36] In clinical surgery practice, the optimum configuration is tested for patient satisfaction before surgery using contact lenses. A similar strategy may be appropriate when applying 1 of the 2 presented ablation profiles including monocular multifocal/aspheric treatment for advanced monovision. Assuming that in the future we will have access to such a set of contacts and the patient may decide to have surgery after a few days of simulation of his or her future optics, there is still a risk for dissatisfaction. In a study testing monovision in presbyopic patients with contact lenses, the immediate response was not a good predictor of satisfaction after 2 weeks.[37]

Table 3. Quality of the retinal image and pupil diameter combinations (GO model, point light source, λ = 550 nm).

	RMS Wavefront Error (µm)	
Pupil Diameters (mm)	Far Distance/5.0 m	Near Distance/0.4 m
5.0/2.5	1.42	0.52
4.0/2.0	1.36	0.38
6.0/3.0	1.36	0.83

RMS = root mean square

A drawback of this theoretical study is its weak relation to clinical reality. The RMS wavefront errors for distant objects for the GO approach, as well as for the CSI approach, are significantly higher than the RMS higher-order wavefront errors in the normal population[38] but for near objects are promisingly close to the normal distribution. There are many other more sophisticated metrics evaluating retinal image quality including metrics predictive of visual performance,[19] in which a neural transfer function filters the retinal image. In addition, the modeling we present does not include the typical higher-order aberrations of the normal presbyopic eye; also, for example, Monte Carlo-simulations using the variety of aberration structures present in the normal population[39] should be performed before testing the aspherical/multifocal techniques in clinical studies.

The last and most critical point is that any presbyopia "correction" is necessarily a kind of compromise. Whatever one wins in the near domain is lost in far distance vision and vice versa. Keeping this in mind, and considering the dependence of the optical result on pupil sizes under various conditions and its centration, it is obvious that any ablative presbyopic correction should be handled as a customized treatment and simulated preoperatively by means of special contact lenses to avoid problems resulting from anisometropia. One of the strongest predictors for a satisfying refractive surgery outcome is the patient's expectation. Especially with presbyopia correction, the balance of the optically possible and the individually desirable must be made preoperatively. Also important in this context is the reversibility of the operation: Simple monovision and GO are easy to correct with a reoperation, but the CSI profile is more difficult to reverse, although progress has been reported using advanced customized ablation with Zernike and Fourier algorithms.[40]

REFERENCES

1. Huber C. Planned myopic astigmatism as a substitute for accommodation in pseudophakia. Am Intra-Ocular Implant Soc J 1981; 7:244–249
2. Schachar RA. Theoretical basis for the scleral expansion band procedure for surgical reversal of presbyopia [SRP]. Compr Ther 2001; 27:39–46
3. Qazi MA, Pepose JS, Shuster JJ. Implantation of scleral expansion band segments for the treatment of presbyopia. Am J Ophthalmol 2002; 134:808–815
4. Mathews S. Scleral expansion surgery does not restore accommodation in human presbyopia. Ophthalmology 1999; 106:873–877
5. Moreira H, Garbus JJ, Fasano A, et al. Multifocal corneal topographic changes with excimer laser photorefractive keratectomy. Arch Ophthalmol 1992; 110:994–999
6. Anschütz T. Laser correction of hyperopia and presbyopia. Int Ophthalmol Clin 1994; 34(4):107–137
7. Ruiz LA, inventor. Apparatus and method for performing presbyopia corrective surgery. US Patent 5 533 997. June 29, 1994

8. King MC, inventor. Correction of presbyopia by photorefractive keratectomy. World Patent 9 325 166. June 10, 1993
9. Nizzola GM, inventor; Nibatec SA, assignee. Equipment for the correction of presbyopia by remodelling the corneal surface by means of photo-ablation. US Patent 5 314 422. November 12, 1991
10. Bauerberg JM. Centered vs. inferior off-center ablation to correct hyperopia and presbyopia. J Refract Surg 1999; 15:66–69
11. Telandro A. Pseudo-accommodative cornea: a new concept for correction of presbyopia. J Refract Surg 2004; 20:S714–S717
12. Cantu R, Rosales MA, Tepichin E, et al. Advanced surface ablation for presbyopia using the Nidek EC-5000 laser. J Refract Surg 2004; 20:S711–S713
13. Liou H-L, Brennan NA. Anatomically accurate, finite model eye for optical modelling. J Opt Soc Am A 1997; 14:1684–1695
14. Moon P, Spencer DE. On the Stiles-Crawford effect. J Opt Soc Am 1944; 34:319–329
15. Netto MV, Ambrósio R Jr, Wilson SE. Pupil size in refractive surgery candidates. J Refract Surg 2004; 20:337–342
16. Baikoff G, Lutun E, Ferraz C, Wei J. Analyse du segment antérieur de l'œil avec un tomographe à cohérence optique. Étude statique et dynamique. J Fr Ophtalmol 2005; 28:343–352
17. Schaeffel F, Wilhelm H, Zrenner E. Inter-individual variability in the dynamics of natural accommodation in humans: relation to age and refractive errors. J Physiol (Lond) 1993; 461:301–320
18. Wilhelm H, Schaeffel F, Wilhelm B. Die Altersabhängigkeit der Pupillennahreaktion. Klin Monatsbl Augenheilkd 1993; 203:110–116
19. Thibos LN, Hong X, Bradley A, Applegate RA. Accuracy and precision of objective refraction from wavefront aberrations. J Vision 2004; 4(4):329–351
20. Seiler T, Reckmann W, Maloney RK. Effective spherical aberration of the cornea as a quantitative descriptor of the cornea. J Cataract Refract Surg 1993; 19:155–165
21. Jacobi KW, Nowak MR, Strobel J. Spezielle Intraokularlinsen. Fortschr Ophthalmol 1990; 87(Suppl):S29–S32
22. Leyland MD, Langan L, Goolfee F, et al. Prospective randomised double-masked trial of bilateral multifocal, bifocal or monofocal intraocular lenses. Eye 2002; 16:481–490
23. Pieh S, Lackner B, Hanselmayer G, et al. Halo size under distance and near conditions in refractive multifocal intraocular lenses. Br J Ophthalmol 2001; 85:816–821
24. Lesueur L, Gajan B, Nardin M, et al. Résultats comparatifs visuals et qualité de vision de deux implants multifocaux; silicone multifocal et PMMA bifocal. J Fr Ophtalmol 2000; 23:355–359
25. Knorz MC, Seiberth V, Ruf M, et al. Contrast sensitivity with monofocal and bifocal intraocular lenses. Ophthalmologica 1996; 210:155–159
26. Haaskjold E, Allen ED, Burton RL, et al. Contrast sensitivity after implantation of diffractive bifocal and monofocal intraocular lenses. J Cataract Refract Surg 1998; 24:653–658
27. Baïkoff G, Matach G, Fontaine A, et al. Correction of presbyopia with refractive multifocal phakic intraocular lenses. J Cataract Refract Surg 2004; 30:1454–1460
28. Kiely PM, Smith G, Carney LG. The mean shape of the human cornea. Optica Acta 1982; 29:1027–1040
29. Holladay JT, Dudeja DR, Chang J. Functional vision and corneal changes after laser in situ keratomileusis determined by contrast sensitivity, glare testing, and corneal topography. J Cataract Refract Surg 1999; 25:663–669
30. Koller T, Iseli HP, Hafezi F, et al. Q-factor customized ablation profile for the correction of myopic astigmatism. J Cataract Refract Surg 2006; 32:584–589
31. Chen CC, Izadshenas A, Rana MAA, Azar DT. Corneal asphericity after hyperopic laser in situ keratomileusis. J Cataract Refract Surg 2002; 28:1539–1545
32. Miranda D, Krueger RR. Monovision laser in situ keratomileusis for pre-presbyopic and presbyopic patients. J Refract Surg 2004; 20: 325–328
33. McDonnell PJ, Lee P, Spritzer K, et al. Associations of presbyopia with vision-targeted health-related quality of life. Arch Ophthalmol 2003; 121:1577–1581
34. Johannsdottir KR, Stelmach LB. Monovision: a review of the scientific literature. Optom Vis Sci 2001; 78:646–651
35. Greenbaum S. Monovision pseudophakia. J Cataract Refract Surg 2002; 28:1439–1443
36. Jain S, Ou R, Azar DT. Monovision outcomes in presbyopic individuals after refractive surgery. Ophthalmology 2001; 108:1430–1433
37. Du Toit R, Ferreira JT, Nel ZJ. Visual and nonvisual variables implicated in monovision wear. Optom Vis Sci 1998; 75:119–125
38. Wang L, Santaella RM, Booth M, Koch DD. Higher-order aberrations from the internal optics of the eye. J Cataract Refract Surg 2005; 31:1512–1519
39. Canales VF, Cagigal MP. Monte Carlo simulation of irradiance distribution on the retina after refractive surgery. J Refract Surg 2004; 20: 384–390
40. Hafezi F, Jankov M, Mrochen M, et al. Customized ablation algorithm for the treatment of central steep islands after refractive laser surgery. J Cataract Refract Surg 2006; 32:717–721